EXTRACTION OF SEAGRASS BIOPHYSICAL PARAMETERS USING UNMANNED AERIAL SYSTEMS (UAS)

Ayin Tamondong[1,2], Anne Glydel Dalagan[1], Lei Anne Manasan[1], Roseanne Ramos[1]
[1]Department of Geodetic Engineering, University of the Philippines, Diliman, Quezon City, Philippines 1101
[2]E-mail: amtamondong@up.edu.ph

KEY WORDS: UAV, mapping, classification, density

ABSTRACT

Carbon dioxide concentration in the atmosphere is drastically increasing every year because of continuous development of industrial activities of today's society. An active research regarding carbon sequestration and carbon storage is progressing, demanding for more investigation and analysis of carbon sinks. Recent studies found out that coastal wetlands – mangroves, saltmarshes, and seagrass, are far more capable of carbon sequestration and carbon storage than terrestrial ecosystems. Approximately 15% of total carbon storage in the ocean are sequestered by seagrasses, although seagrasses inhabit only 0.2% of the area of the oceans. To estimate the carbon sequestered by seagrasses, extent, percent cover and density are among the biophysical parameters necessary. In this study, the RGB aerial images using Unmanned Aerial System (UAS) was utilized for classification of seagrass and extraction of seagrass density and percent cover. UAS survey was conducted in Anda, Pangasinan to gather RGB images and field samples were also collected. The images were mosaicked to produce an orthophoto. To classify seagrass from non-seagrass areas, object-based classification (OBC) and pixel-based classification (PBC) were used and compared by implementing the Support Vector Machine (SVM) and Maximum Likelihood method. Mixture Tuned Matched Filtering was performed for the derivation of the percent cover and density. Results showed that OBC having an overall accuracy of 93% produced higher accuracy than PBC which yields 86%. Meanwhile, most seagrass areas were categorized with dense and continuous density. The study proved that Unmanned Aerial System (UAS) was an effective approach for seagrass cover mapping because it produces high-resolution images resulting to more accurate maps.

INTRODUCTION

Seagrasses are fully submerged marine plants that grow in sediments and produce flowers, pollen, and seeds located below the coastal ocean. Like terrestrial plants, they also rely on sunlight for growth and sustainability which penetrates through the seawater (ChMura, 2016). Seagrass meadows play a significant role in the equilibrium of ecosystem by providing habitat and food source to ocean creatures (Unsworth and Cullen, 2010) and assists in creating favorable habitat by filtering water to improve water clarity and trapping suspended sediments (van der Heide et.al., 2007). However, recent studies show that there is 0.9% per year global declination (net loss rate) in seagrass due to the stresses caused by human activities (Waycott et al. 2009 cited in Marba, 2015). In the Philippines, about 30% to 40% of seagrass cover has been lost for the past 50 years. Loss of seagrass cover has a great impact in ecological and economical aspects that's why it is important to estimate and assess the current state of seagrass resources.

In order to estimate these resources, remote sensing techniques can be utilized as it can cover large areas in a short period of time. One popular remote sensing technique well-suited for acquiring information in benthic ecosystem is the Unmanned Aerial System (UAS), a remote-controlled aircraft flown for reconnaissance, mainly used for military applications but also employed to obtain remotely sensed imagery for research involving natural disaster monitoring, biodiversity observations and vegetation measurements in forests or underwater. It is also proven to provide precise measurements of submerged aquatic vegetation in shallow waters having low turbidity (Flynn et. al., 2014). Delivering high-resolution remotely-sensed data in low flying height makes it easier to observe for changes and dynamics of the area of interest. Hence, UAS is a powerful tool which may be used for seagrass cover mapping and extraction of percent cover and density.

This objective of this study is to examine the potential of using Unmanned Aerial System (UAS) for seagrass cover mapping and determination of biophysical parameters such as percent cover and density.

METHODOLOGY

The study was conducted in Anda, Pangasinan, specifically in the coastal waters near shore Siapar Island (16°21'19.64" N, 119°57'6.88" E) in Northwestern Philippines as shown in Figure 1. The areas covered generally had clear and shallow waters. Aquaculture structures (specifically oyster farms) are also present in the study site.

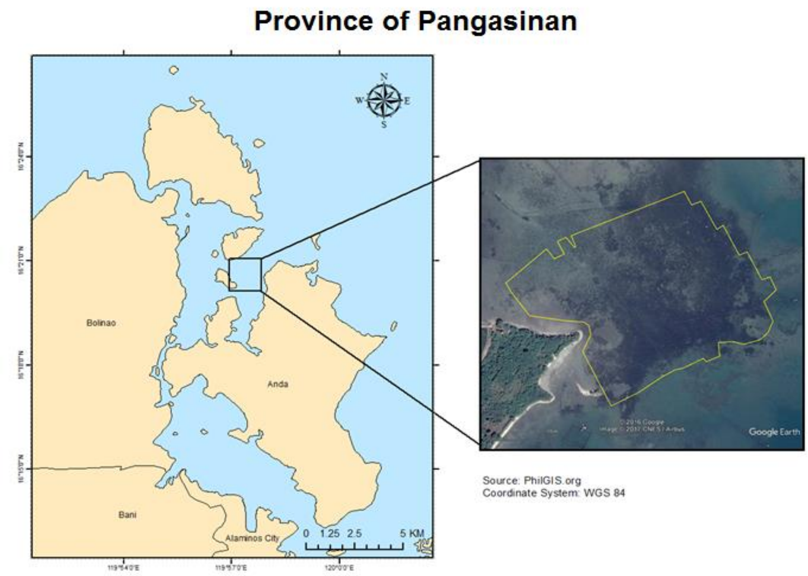

Figure 1. Location of seagrass study site in Siapar Island, Anda, Pangasinan

Since UAS utilizes optical sensors thus, limited in submerged aquatic ecosystems, the survey was conducted during low tide (-0.3 m below mean sea level) with average natural illumination in order to avoid solar glare and irradiance and to capture maximum surface objects during flights. The flight plans were created using Pix4D Mapper software. Both DJI Phantom 3 and DJI Phantom 4 quadcopters with RGB cameras were used to capture the totality of the study area. From the flight plan created, the UAS flew over the study area in five flight trials at different altitudes: 30 m and 80 meters using DJI Phantom 3 and DJI Phantom 4. Field sample points were collected systematically by capturing photos and taking the coordinates using Garmin Monterra handheld GPS every 15 steps as seen in Figure 2 for data validation. The device used has a horizontal accuracy of 3 meters to 10 meters. A total of 132 photos were captured at the site.

Figure 2. Collecting of ground truth samples from the field

Images gathered from the UAS were mosaicked into an orthophoto using the software Agisoft Photoscan Professional through the five steps illustrated in Figure 3. The seven orthophotos were compared visually so that the orthoimage that would be chosen displays minimal sun glint over the study site. Flight 4+5 was selected among all images because it produced the least sun glint in most parts.

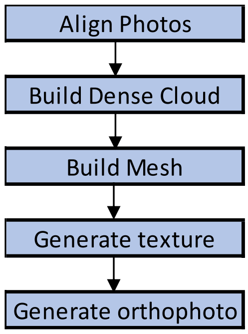

Figure 3. Workflow of generating orthophoto

To remove unnecessary and erroneous areas (e.g. areas covered with sun glint & land), the orthoimage derived from the merged photos of 4th and 5th flights was masked by digitizing the selected area of interest. Field samples were geotagged using ArcGIS to be used as ground truth samples which were then overlaid and tagged into the new orthoimage. There were 132 samples collected from selected parts in the field.

For pixel-based classification, region of interests (ROI) for two classes, seagrass and non-seagrass were selected using ENVI. A total of 285 training samples were created for seagrass class whereas 287 ROIs were chosen for non-seagrass areas. Afterwards, maximum likelihood was performed on the image using the said classes with the training samples. Maximum likelihood classification worked by calculating the probability that a pixel was part of a certain class with the assumption that each band has a normal distribution. Resulting classification was further polished by clumping classes to smoothen the classification image and to reduce the salt-and-pepper noise. A sample area from the orthophoto and the results of the classification is shown in Figure 4.

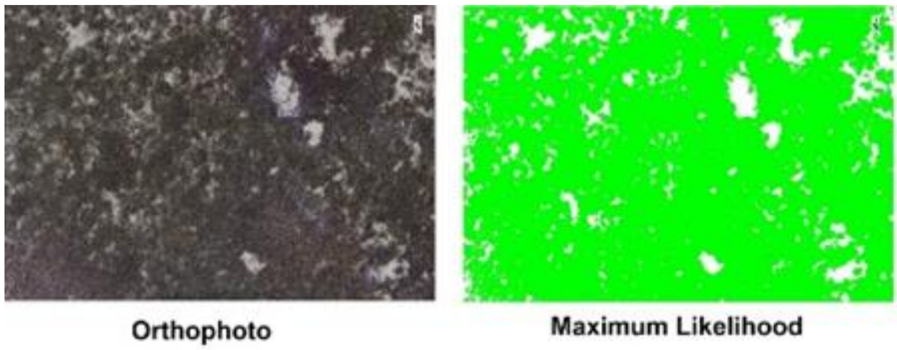

Figure 2. Screenshot of orthophoto and result of maximum likelihood classification of a sample area

For object-based classification, the software used was eCognition Developer 9. The orthoimage was loaded and a multi-resolution segmentation process was implemented. The parameters used for segmentation are shown in Table 1. These parameters were chosen after several iterations of the process.

Table 1. Parameters for segmentation

Scale	100
Shape	0.3
Compactness	0.7

Table 2. Parameters for SVM

Kernel type	Radial Basis Function
C	17
γ	0.05

From the objects created from segmentation, samples for seagrass and non-seagrass classes were selected from the image. These training samples were the same set used for the pixel-based classification. After selection of samples, the image object level was trained using the classifier Support Vector Machines (SVM). Support Vector Machine (SVM) was used to determine the optimal separating hyperplane that would give the maximum space between the classes by utilizing the training datasets that were selected from the edge of descriptors (support vectors) and discarding other training data (Tzotzos, n.d.). Table 2 indicated the kernel and parameters used which produced the most satisfactory results. Then, the classifier was applied and performed to the image to derive the object-based classification image as seen in Figure 5. For accuracy assessment, the ground truth samples used were the same in both classification methods.

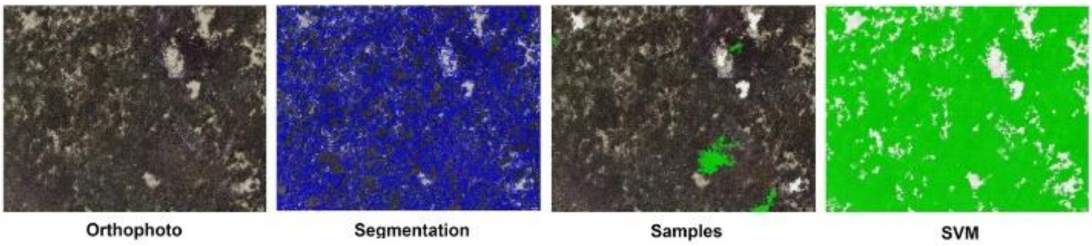

Figure 5. Samples of intermediate outputs in object-based classification

For the estimation of percent cover, Mixture Tuned Matched Filtering (MTMF) was employed, a process of mixed pixel classification wherein the subpixel abundance of the element of interest would be estimated and background noise would be removed (Mitchell et.al., 2009). Matched filtering worked by mapping and estimating the abundance of endmembers defined by the user using a partial unmixing technique. Higher infeasibility values pixels would most probably be MF false positives. Correctly mapped pixels would have an MF score above the background distribution around zero and a low infeasibility value. (Blanco et. al., n.d.)

First, noise estimates were computed in order to remove noise from the background. Forward minimum noise fraction (MNF) transformation was applied to the orthoimage after calculating noise statistics during the process. At the least, two output bands were selected to produce the final MNF transformed image. A single endmember, should be in MNF spectra, was needed in MTMF which was used as a reference datum in order to estimate the relative match of pixel values. Supposedly, pixel purity index (PPI) should be determined first to filter the purest pixels from the image, however, in this case, the user performed the selection of the desired endmember because the input file was a high-resolution image. MTMF utilized both MNF transformed image and endmember to perform matched filtering (MF) which produced an MF image accompanied with an infeasibility image.

Foliar cover from 45 ground samples was estimated using the GPS photos acquired during fieldwork as shown in Figure 6. Average area covered by all photos was estimated to have a length of 0.5m and width of 0.38m then projected into the orthoimage using fishnets to estimate the average MF score of each sub-area. The relationship between both parameters was determined using linear regression.

90% 65% 70%

Figure 3. Photos of ground truth samples and their corresponding cover (%) estimation.

RESULTS AND DISCUSSION

Observed land areas and water areas with visible spectral light reflection were clipped out and masked off from the original photo. The final masked orthophoto is shown in Figure 7 which is used for classification and computation of Mixture Tuned Matched Filtering. Noticeably, some seagrass areas in the image, especially in the lower central portion, exhibited a loss in spectral information due to visible sun glint covering these areas. No correction was performed to remove this sun glint since the image consists of three bands (RGB) only. A near infrared (NIR) band was significant for removing this type of noise.

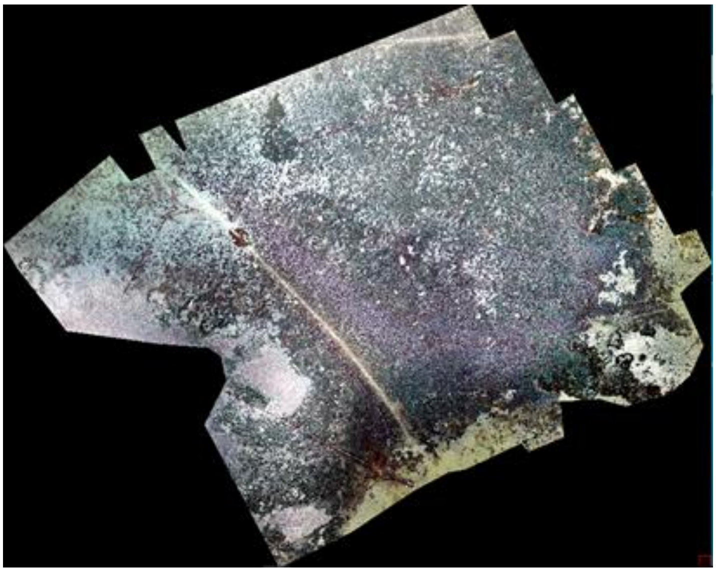

Figure 7. Final masked orthoimage of Flight 4+5 in Siapar Island.

The classification maps of seagrass using maximum likelihood and support vector machine are shown in Figure 8. The final classification image of maximum likelihood showed some salt-and-pepper noise in some areas even though smoothing was already performed from the original classification result. On the other hand, SVM classification showed better result visually.

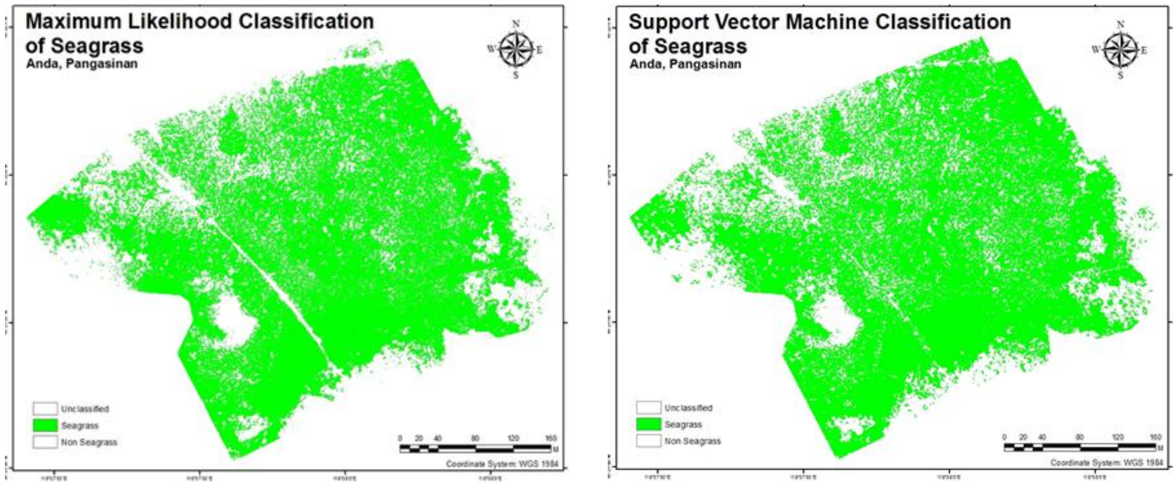

Figure 8. Maps of seagrass using maximum likelihood classification and support vector machine

Comparing the two methods visually, it was observed that a small portion in the western part of the classification results for both methods was not accurately classified in which the seagrass clusters should be sparse based on the original image. Nonetheless, SVM classification provided better appearance from Maximum Likelihood classification on the said region wherein the non-seagrass areas were overestimated to be seagrass areas. Moreover, SVM accurately classified the seagrass areas on the extents especially on the upper part of the image in which Maximum Likelihood failed to achieve. On the other hand, seagrass in the center portion was classified correctly by SVM based from the original orthophoto. However, due to the sun glint evident on the original orthophoto, some seagrass areas were classified as non-seagrass. Nevertheless, SVM visually exhibited more accurate of seagrass cover as presented in Figure 9.

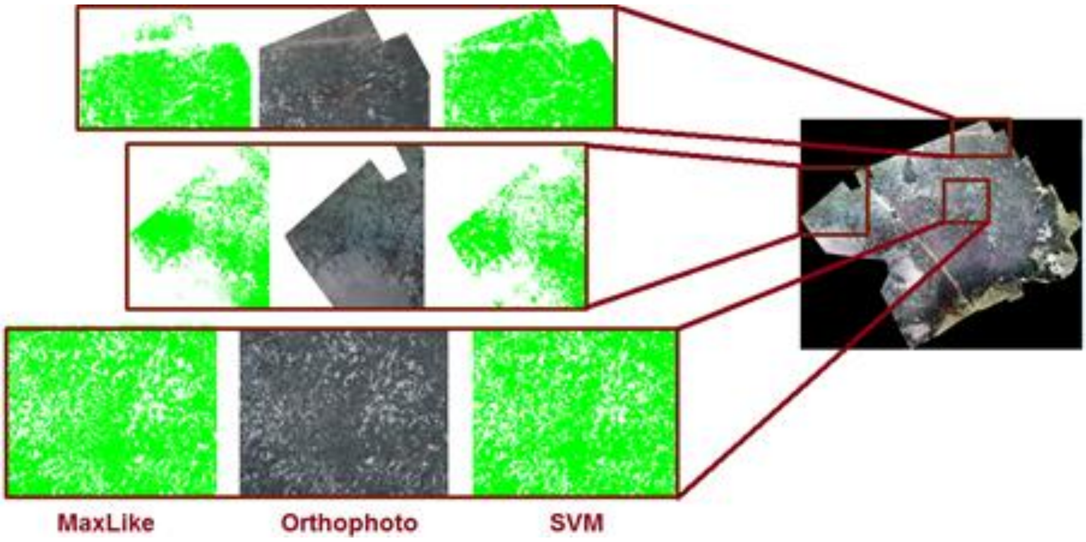

Figure 4. Visual comparison between maximum likelihood and SVM classification

Results of the pixel-based and the object-based classification of the RGB image were compared from the set of ground truth samples created randomly over the image. Confusion matrices were computed for both maximum likelihood and SVM classification approaches as shown in Table 3 indicating the overall accuracy, kappa statistics and percentages of correctly and wrong classified pixels of each class. It was clearly shown that SVM classification has higher accuracy than maximum likelihood classification by 7.29%. Furthermore, the agreement between the ground truth samples and from SVM classification result (κ=0.8645) had evidently higher value compared to maximum likelihood classification result (κ=0.7135). The overall accuracy of maximum likelihood classification was largely influenced by the omission and inclusion of non-seagrass areas into the classification. For SVM, the primary source of error was the classification of some non-seagrass areas into seagrass class.

Table 3. Confusion matrices of maximum likelihood and SVM classification

	Support Vector Machine	Maximum Likelihood
Overall Accuracy (%)	93.3106	86.0248
Kappa Coefficient	0.8645	0.7135
Users Accuracy (%)		
Seagrass	97.42	87.86
Non-seagrass	88.49	83.51
Producer's Accuracy (%)		
Seagrass	90.84	87.86
Non-seagrass	96.70	83.51

Overall, SVM exhibited higher accuracy and precision for the classification of seagrass cover. Since object-oriented classification resembled a manually digitized map, the approach was able to highlight detailed features of the objects whereas, pixel-based classification misclassified areas displaying white tiny dot noises over the image. Even though sample selection and classification was easier and faster by using object-based classification (OBC), it definitely had longer total processing time, especially if the processing unit used had lower specifications because of the tedious segmentation procedure. The main advantage of using OBC is that it enables the extraction of classification attributes (texture, area, class names, etc.) which is very efficient especially when dealing with more rigorous and extensive classification.

For MTMF, the eigenvalues of each input bands were displayed where the 2 bands with the highest eigenvalues were selected to produce the MNF transformed image. Bands with eigenvalues greater than 1 contained significant data while those with less than 1 contained predominantly of noise. The MF image produced by MTMF was shown in Figure 10a where light pixels indicate high MF score while dark pixels correspond to negatively matched pixels. Light pixels in infeasibility image in Figure 10b signified incorrectly mapped pixels or false positives which were integrated with MF image to reduce the error of spectral mapping.

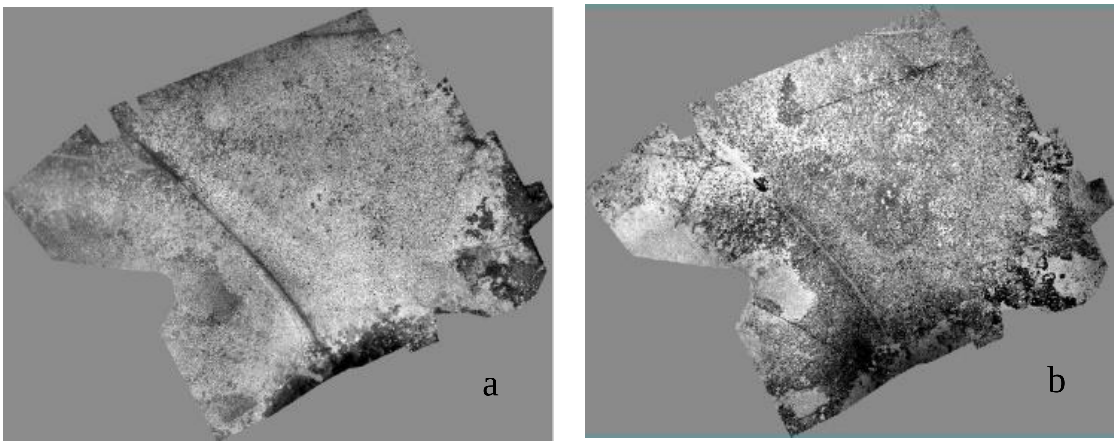

Figure 10. MTMF output with (a) MF fraction image and (b) infeasibility image

In order to compensate for the difference in resolution of orthoimage and GPS photos, fishnets of 22x16 pixels were created around each of the 45 samples to compute the average MF score per ground truth samples. All negative values were disregarded while relatively low pixels were also excluded from analysis. Linear regression of both parameters was determined to identify whether their relationship was significant. Figure 11 shows that MF score and foliar percent cover were moderately correlated to each other based from its $R^2 = 0.5751$.

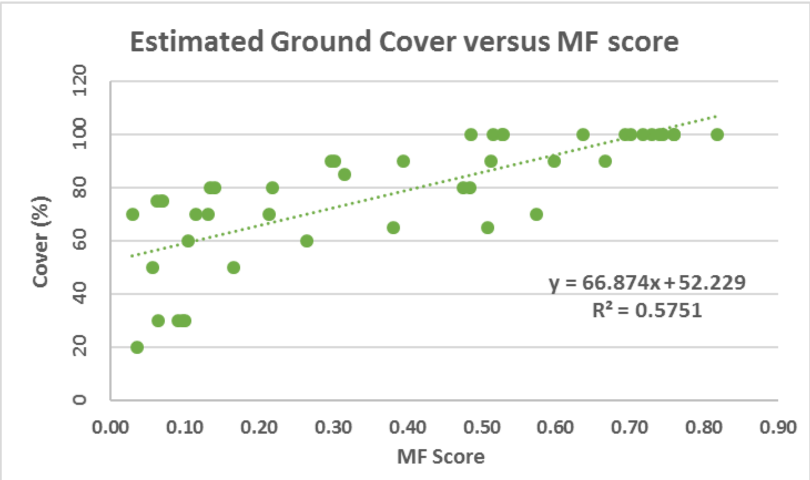

Figure 11. Linear regression analysis of MF score and estimated percent cover

The linear regression model was used to estimate the foliar cover of the full scene of MTMF output of the study area. Afterwards, the density was computed per pixel where the result was classified into different categories. Negative values and background pixels were already excluded from the classification. Values beyond 100% were considered to belong to the same Seagrass foliar cover was classified into 0-15%, 15-45%, 45-75%, 75-95%, and 95-100% corresponding to very sparse, sparse, moderate, dense, and continuous patches. It can be seen in Figure 12 that it was covered predominantly by continuous patches, especially in the lower middle region. Seagrass cover in the upper right portion of the image was varying from sparse to moderate while very few parts were considered very sparse. Overall, the map was able to represent the actual seagrass features from the original orthoimage.

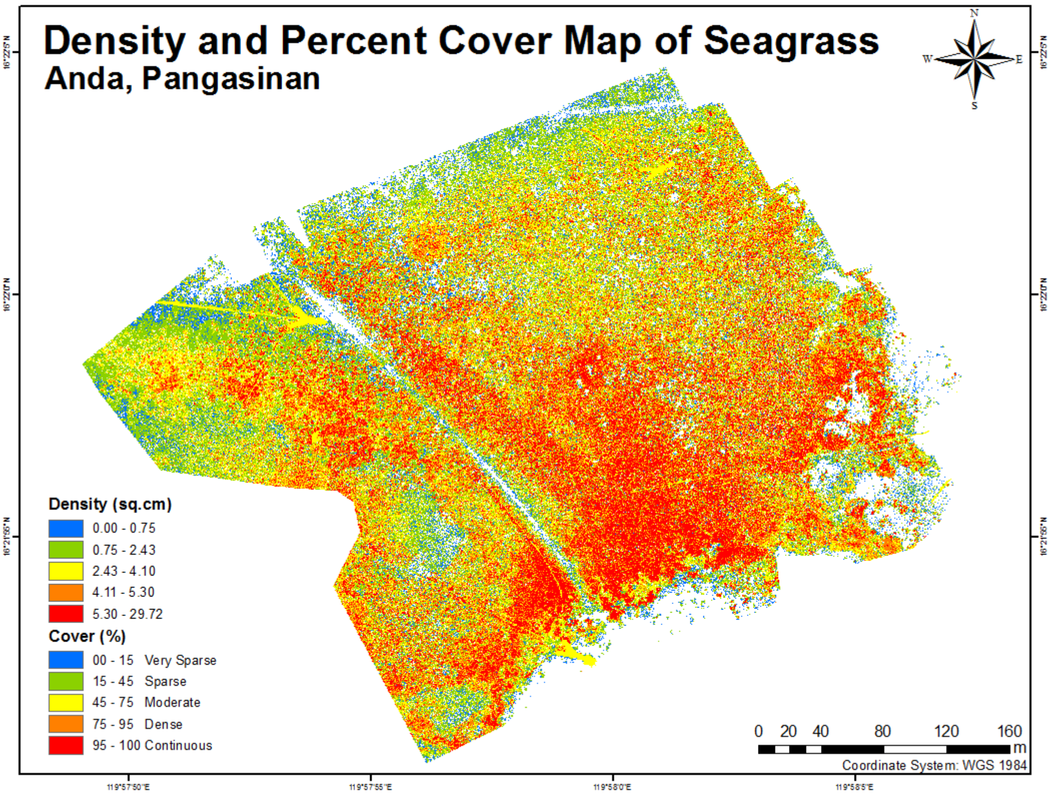

Figure 12. Density and percent cover map of seagrass meadows in Siapar Island

CONCLUSION

Object-based classification (OBC) provides better classification results compared to pixel-based classification in mapping seagrass cover using RGB aerial images based on the obtained confusion matrices. Moreover, OBC has the advantage in terms of appearance because it accurately delineates the irregular shapes of seagrass unlike the smooth edges displayed by PBC. Thus, OBC approach specifically, Support Vector Machine classifier can be used for classification of high-resolution images. However, if high accuracy is not imperative, pixel-based classification (specifically maximum likelihood) may be executed considering that it can also provide acceptable performance.

The use of MTMF method is more appropriate for coarse pixels or low-resolution image as it performs spectral “unmixing” and classifies the components into different categories. When dealing with high-resolution data, indeed, MTMF is not necessary for spectral analysis because its pixels are relatively pure and identifiable. However, this study proved that MTMF can still perform well and produce good classification map for benthic species like seagrass.

Hence, Unmanned Aerial System (UAS) is an effective approach for seagrass cover mapping because it produces high-resolution images resulting to more accurate maps. Providing high spatial resolution imagery while being inexpensive, UAS is a promising tool for extraction of biophysical parameters, specifically percent cover and density.

Classification and spectral mapping outputs can be further improved provided that more ground truth samples are obtained evenly from all parts of the study area and foliar percent cover estimates of seagrass shall be done directly from the field to ensure accuracy and consistency of estimation. In line with this, instruments to be used such as handheld GPS shall have better accuracy to reduce the difference in spectral resolution between data generated from other sources like UAV. Additionally, ground control points (GCPs) can be established to perform accurate georeferencing between various datasets.

ACKNOWLEDGEMENTS

The authors would like to thank the Department of Science and Technology for funding this research and dissemination. We would like to show our gratitude to Engr. Jore Montelibano for lending his expertise on Unmanned Aerial System (UAS) during the data acquisition.

REFERENCES

Blanco, A., Tamondong, A., Tagle, E., Fortes, M., Nadaoka, K. Change in Seagrass Fractional Cover in Bolinao and Anda, Philippines Derived from Landsat Images.

Chmura G, Shoart F, Torio D, Arroyo-Mora P, Fajardo P, Hatvany M, van Ardenne L. (2016) North America's Blue Carbon: Assessing Seagrass, Salt Marsh and Mangrove Distribution and Carbon Sinks. Commission for Environmental Cooperation

Coulloudon, Bill, and Kris Eshelman. Sampling Vegetation Attributes. Denver, Colorado: Bureau of Land Management: National Applied Resource Sciences Center, 1999. PDF.

Flynn, K., & Chapra, S. (2014). Remote Sensing of Submerged Aquatic Vegetation in a Shallow Non-Turbid River Using an Unmanned Aerial Vehicle. Remote Sensing, 6(12), 12815-12836. doi:10.3390/rs61212815

Liu, D., & Xia, F. (2010). Assessing object-based classification: advantages and limitations. *Remote Sensing Letters,1*(4), 187-194. doi:10.1080/01431161003743173

Marbà, N., Arias-Ortiz, A., Masqué, P., Kendrick, G. A., Mazarrasa, I., Bastyan, G. R., Duarte, C. M. (2015). Impact of seagrass loss and subsequent revegetation on carbon sequestration and stocks. Journal of Ecology, 103(2), 296-302. doi:10.1111/1365-2745.12370

Maximum Likelihood. (n.d.). Retrieved May 29, 2017, from https://www.harrisgeospatial.com/docs/MaximumLikelihood.html

Mitchell, J & Glenn, N. (2009). Subpixel abundance estimates in mixture-tuned matched filtering classifications of leafy spurge (Euphorbia esula L.). International Journal of Remote Sensing, vol. 30, no. 23, pp 6099-6119.

The Jornada: Unmanned Aircraft Systems (UAS) for Remote Sensing. (n.d.). Retrieved December 16, 2016, from http://jornada.nmsu.edu/remote-sensing/uas

The UAV - The Future of the Sky. (n.d.). Retrieved December 16, 2016, from http://www.theuav.com/

Tzotsos, A. (n.d.). A Support Vector Machine Approach For Object Based Image Analysis.

Unsworth RK, Cullen LC (2010) Recognising the necessity for Indo-Pacific seagrass conservation. Conservation Letters 3: 63-73